OMTN, Volume *32*

Supplemental information

Silencing of microRNA-106b-5p prevents doxorubicin-mediated cardiotoxicity through modulation of the PR55α/YY1/sST2 signaling axis

Antonio Lax, Fernando Soler, Maria Josefa Fernandez del Palacio, Silvia Pascual-Oliver, Miriam Ruiz Ballester, Jose Javier Fuster, Domingo Pascual-Figal, and Maria del Carmen Asensio-Lopez

METHODS AND RESULTS EXPANDED

Methods

Protein extraction. Fresh LV (~30 mg) from myocardium tissue or harvested untreated or treated cells. (~ 8 × 10^6 cells), were washed using cold DPBS and gently homogenized in lysis buffer by sonication and then centrifuged at 20,000 ×g at 4 °C, for 20 min. The lysis buffer was composed of: 150 mM Tris–HCl, 1 mM EGTA, 1% Triton X-100, 1% sodium deoxycholate, and 0.1% SDS, pH 8.0] along with 100-fold diluted protease and phosphatase inhibitors. The resulting supernatant was aliquoted and frozen at −80 °C. Protein concentrations were determined by the bicinchoninic acid method[1].

Subcellular fractionation. Experimental protocols for the isolation of nuclear and cytosolic fractions from hiPSCMs and tissue were based on the experimental protocols described previously[2], with some modifications. Briefly, fresh LV (~ 30 mg) tissue or harvested untreated or treated cells (~3 × 10^6 cells) were washed using cold DPBS along with 100-fold diluted protease and phosphatase inhibitors. Human cardiomyocytes were pelleted by centrifugation at 480 ×g for 10 min at 4 °C, while the myocardium was placed in a pre-chilled glass Petri dish and minced on ice using sharp scissors. All samples were homogenized in 500 µl of STM buffer at pH 7.4, containing 250 mM sucrose, 50 mM Tris-HCl, 5 mM $MgCl_2$, 5 mM Na_3VO_4, 1% (v/v) protease and phosphatase inhibitor cocktails and homogenized for 1 min on ice using a tight-fitting Teflon pestle attached to a Potter S. homogenizer (Sartorius Stedim, Goettingen, Germany) set to 800 rpm. The homogenate was maintained on ice for 30 min, vortexed at maximum speed for 15 s, and then centrifuged at 800 ×g for 15 min at 4 °C. The pellet was labeled as P0 and kept on ice; the supernatant was labeled as S0. The pellet P0 (containing nuclei and debris) was resuspended in 500 µl STM buffer, vortexed at

maximum speed for 15 s, and then centrifuged at 500 ×g for 15 min at 4 °C. Following the above step, the nuclear pellet was labeled as P1 and kept on ice, and the supernatant S1 (cell debris) was discarded. To further increase the purity of the P1 fraction, it was washed in 400 µl STM buffer, vortexed at maximum speed for 15 s, and then centrifuged at 1000 ×g for 15 min at 4 °C. The washed pellet was labeled as P2 (S2 was discarded) and resuspended in 100 µl NET buffer composed of 20 mM Hepes pH 7.9, 1.5 mM $MgCl_2$, 0.5 M NaCl, 0.2 mM EDTA, 20% (v/v) glycerol, 1% (v/v) Triton-X-100 and protease and phosphatase inhibitors, using a pipette to triturate until homogeneity. Pellet P2 was vortexed at maximum speed for 15 s and incubated on ice for 30 min; the resulting fraction contained the nuclei, which were lysed by sonication (Soniprep 150, MSE, London, UK) at a high setting for 10–15 s with 30 s pauses while being kept on ice. The lysate was centrifuged at 9000 ×g for 30 min at 4 °C, and the resultant supernatant (S3) was the final "nuclear fraction." Cytosolic fractions were extracted from S0 by centrifugation at 11,000 ×g for 10 min at 4 °C. The supernatant contained the cytosol fraction. The protein content of each compartment was determined using a BCA protein assay[1].

Detection of protein-Western blotting. The separation and detection of proteins were performed by standard procedures, as previously described[3]. Aliquots of soluble protein (15 µg) [total protein or subcellular fractions] were initially boiled for 6 min in SDS gel-loading buffer and then, equal amounts of protein were resolved on 8% or 10% SDS–polyacrylamide gels[3] and electroblotted at 4 °C on PVDF membrane using a wet transfer system apparatus from Bio-Rad in presence of methanol for 1 h at 100 V. To evaluate high molecular weight proteins, the electroblotted experimental conditions changed to overnight at 4 °C, 25 V and in absence of methanol. The transferred filters

were blocked for 1 h at room temperature with 5% BSA (w/v) in TBST (137 mM NaCl, 20 mM Tris and 0.1% Tween-20, pH 7.6) followed by an overnight incubation at 4 °C with primary antibody into blocking buffer. Primary antibodies and their dilutions, sources, and references are summarized in the main manuscript. Equal loading in the lanes was checked with the GAPDH or TBP antibodies, markers of the cytosol and nuclear fractions, respectively. Then, the membranes were washed five times for 10 min each with TBST and incubated for one hour at room temperature with appropriate secondary antibodies (ECL Mouse IgG, HRP-linked whole Ab (NXA931) or ECL Rabbit IgG, HRP-linked whole Ab (NA934)) from Amersham BioSciences, diluted in blocking buffer at 1:10,000. After this, the membranes were washed five times for 10 min each with TBST and immunoreactive bands were detected by ECL (Amersham ECLTM Primer Western Blotting Detection Reagent (GE Healthcare, NJ, USA) (RPN2232), using a ChemiDoc XRS+ system with Image Lab software from Bio-Rad Laboratories (Berkeley, CA, USA). A quantitative analysis was performed with Gel-Pro Analyzer 3.1 software (Sigma). See BlueTM Plus2 Prestained protein standard (LC5925) from Life technologies or Precision Plus ProteinTM Dual Colour Standards (1610374) from BioRad were used as Prestained Protein Markers.

PP2A phosphatase assay. To measure PP2A phosphatase activity, we used a PP2A Immunoprecipitation Phosphatase Assay Kit (Millipore Sigma, catalog number 17-313). In brief, cells were lysed in 20 mM imidazole HCl, 2 mM EDTA and 2 mM EGTA, pH 7.0 with 10 µg/mL each of aprotinin, leupeptin and pepstatin, 1 mM benzamidine and 1 mM PMSF. The lysates (2 mg) were then immunoprecipitated with 2 µg of anti-STRN4 antibody (Abcam, ab177155) and 40 µl of protein-A-agarose beads at 4 °C overnight. The beads were washed three times with lysis buffer followed by Ser/Thr assay buffer.

The phosphatase reactions were then performed in Ser/Thr assay buffer with a final concentration of 750 μM of MAP4K4 phosphopeptides: S771/ S775 (A-A-S-pS-L-N-L-pS-N-G-E-T-E-S-V-K), S876 (L-T-A-N-E-T-Q-pS-A-S-S-T-L-Q-K) or S1251 (V-F-F-A-pS-V-R-S) for 10 min at 30 °C. To provide evidence that the immunoprecipitated phosphatase activity was PP2A, we treated parallel immunoprecipitates with 5 nM okadaic acid (Cell Signaling, #5934). Dephosphorylation of the phosphopeptide was measured through malachite green phosphate detection at 650 nm using a microplate reader, CLARIOstar Plus (BMG Labtech).

Luciferase reporter assay. To confirm that *miR-106b-5p* targets the 3′-UTR of *PR55α*, we cloned the region of *PR55α* 3′-UTR, which contains the predicted *miR-106b* binding sites, into a pGL14 Luciferase reporter vector (*Luc-PR55α-WT*; PROMEGA, Madison, WI, USA). Luc-PR55α-mutant (*Luc-PR55α-Mut*) was also constructed, which contained a mutated *PR55α* at the binding site of *miR-106b* (5′- GCACUUU-3′ mutated to 5′- CGUUUAAA-3′) using an In-Fusion cloning kit (CLONTECH, Mountain View, CA, USA), as per the manufacturer's protocol. The Dual-Luciferase Reporter Assay System was applied for the luciferase reporter assay (PROMEGA). HEK 293T/17 cells (ATCC) were simultaneously transfected with wild-type (wt) or mutant-type (mut) 3′-UTR PR55α and miR-106b mimic or NC mimic. Luciferase activity was detected using a CytoFLEX Flow Cytometer (BECKMAN COULTER). Firefly luciferase activity was normalized to Renilla luciferase activity. The ratio of PR55α 3′-UTR to the NC mimic was set as 1; therefore, the displayed results indicate the fold changes relative to the control. The experiments were performed three times in triplicate.

Co-immunoprecipitation protocol. For co-immunoprecipitation, 400 µg of nuclear extracts from the cells (8×10^6 cel) or the left ventricular area was collected and incubated overnight only in the presence of an antibody to HDAC4 (CELL SIGNALING, 5392, 1:100) or YY1 (CELL SIGNALING, 2185, 1:500) at 4 °C with gentle shaking. After this, 20 µl of protein A–Sepharose slurry was added and the samples were incubated for 4 h at 4 °C with gentle shaking. The beads were then washed three times with IP buffer (20 mM HEPES pH 7.4, 0.5 mM EDTA, 150 mM NaCl, and 0.1% Triton X-100) to remove non-specific binding. For each wash, the beads were mixed gently with IP buffer and centrifuged at 4 °C, and the supernatant was discarded. The antigen–antibody complex was eluted from the beads by heating the samples in 25 µl 1× SDS gel-loading buffer for 4 min. To analyze the immunoprecipitate by western blot, the samples were loaded into a continuous SDS-PAGE gel and run at a 30 mA constant current for 2 h. The interaction was analyzed by western blotting using primary antibodies to HDAC4 (CELL SIGNALING, 5392, 1:1000) or YY1 (CELL SIGNALING, 2185, 1:1000). As a control, we used IgG.

Levels of c-TnT, LDH, MDA, Epinephrine and sST2 in serum and/or cell culture media. The concentrations of each cited molecule in serum and the cellular supernatant were measured using the ELISA procedure. Lactate Dehydrogenase Kits for humans (MBS009535) and mice (MBS2022204) as well as ELISA kits to measure the levels of sST2 or c-TnT (MBS262307) were obtained from MYBIOSOURCE.COM. From Abcam, we obtained an MDA Assay Kit (ab238537). From NOVUS biologicals, we obtained an Epinephrine ELISA kit (KA1882). In all cases, the reaction was terminated using a stop solution, and the absorbance was determined at 450 nm using a microplate

reader (CLARIOstar, BMG LABTECK, Ortenberg, Germany). The intra- and inter-assay precisions globally were ≤ 10%.

Tissue distribution and safety assays. To determine the biodistribution of *AM106b*, fluorescently labeled *AM106b* sequences were acquired from Bionova (5′-56-FAM-AM106) and intravenously administered to C57BL mice. The mice were grouped with three animals per group, and the study was repeated three times. While mice in Group 1 were treated with 6 mg/kg *AM106b* and sacrificed after 24h, the animals included in Group 2 and Group 3 were treated using the same dosage of *AM106* but sacrificed after 3 and 6 days after *AM106b* treatment, respectively. The heart, kidneys, liver, lungs, and spleen were collected at sacrifice. As detailed in previous studies with modifications[4], the tissues (100 mg) were homogenized on ice in 1 mL phosphate-buffered saline and diluted 100 times. The resulting diluted homogenates were analyzed using a microplate reader (CLARIOstar Plus) at excitation and emission wavelengths of 488 nm and 525 nm, respectively. The data were normalized with the control mice, which were tissue from mice treated with only saline (Group 4) [The background fluorescence from these tissues was subtracted from the experimental tissue fluorescence readings to exclude the effect of autofluorescence]. The percentage *AM106b* detected was expressed as the ratio of the fluorescence unit of each tissue relative to the sum of fluorescence units of all tissues analyzed and graphically illustrated in Figure S8. To test whether *AM106b* has a toxic effect on tissues, formalin-fixed paraffin-embedded tissues were stained with a standard hematoxylin and eosin stain for histopathologic analysis. Briefly, sections were deparaffinated and rehydrated, stained with Harry′s acidified hematoxylin and alcoholic eosin (Epredia, Kalamazoo, USA), dehydrated, cleared and permanently mounted. Sections were then x400 digitalized (Pannoramic MIDI-II digital slide scanner, 3D

Histech, Budapest, Hungary) and examined with specialized software (Slide Viewer Ver. 2.6.0.166179, 3D Histech). Representative images were obtained by using the same software.

Results

1.- *AM106* treatment leads to a 54% (hiPSCMs exposed to Dox; panel a) or 56% increase (LV myocardium; panel b) in *FOG2* mRNA levels after Dox treatment for 15 h when compared to the groups treated with *antimiR-Ctrl*.

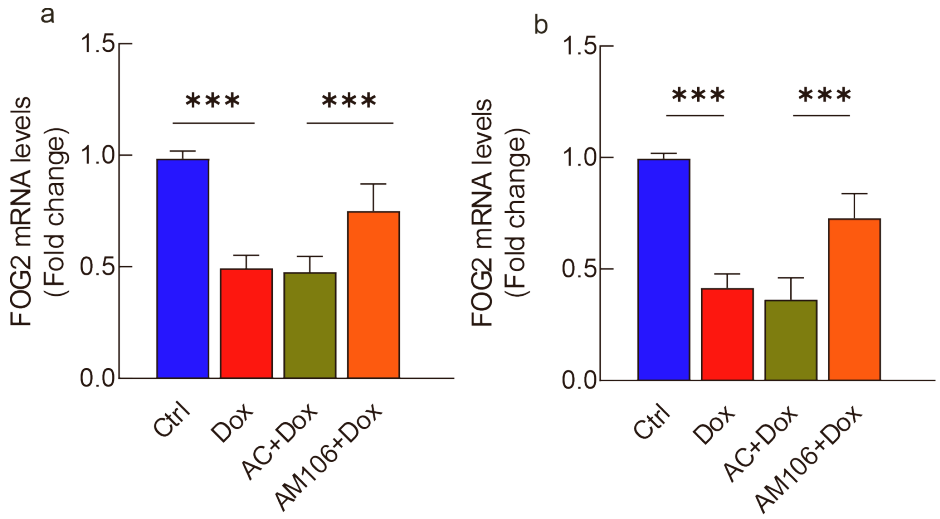

Figure S1.

AM106 treatment increases FOG2 mRNA levels in hiPSCMs and LV myocardium obtained from mice in the presence of Dox. Quantitative real-time PCR analysis of *FOG2* (normalized to GAPDH) in hiPSCMs (a) or mice (b) in presence of Dox. All quantifications are derived from n = 5 independent assays/group. All quantitative data are presented as mean ± SEM. ***p < 0.001 determined by one-way ANOVA followed by post hoc tests with Bonferroni correction. Abbreviations: *AC: antimiR-control; AM106: antimiR-106b*; Ctrl: control; Dox: doxorubicin; *GAPDH*: Glyceraldehyde-3-Phosphate Dehydrogenase.

2.- Gene expression and protein levels of total HDAC4 were analyzed by quantitative real-time PCR and western blot (Figure S2). Compared to the control group, Dox treatment resulted in a significant increase in *HDAC4* mRNA levels ($p<0.001$) which was not prevented by *AM106b* (Figure S2a). These results were confirmed by assessing HDAC4 protein level (Figure S2b).

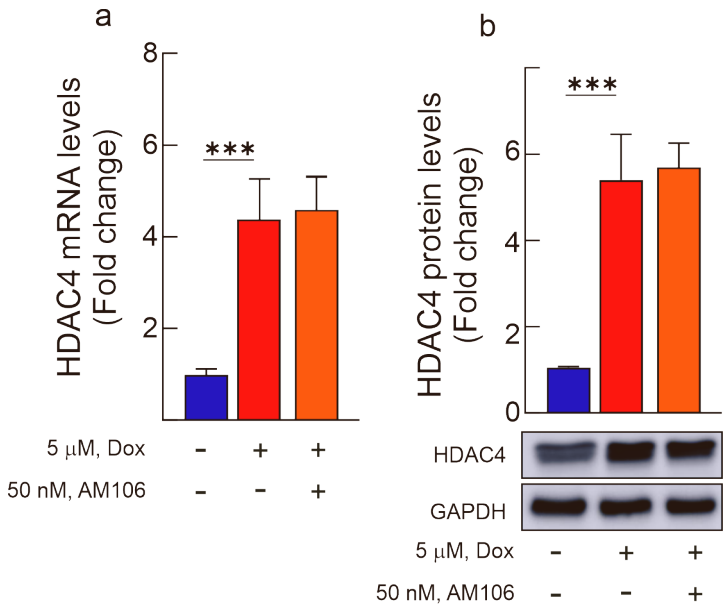

Figure S2.

AM106 treatment did not affect Dox-induced HDAC4 up-regulation. (a) Quantitative real-time PCR analysis of *HDAC4* (normalized to GAPDH) in hiPSCMs. (b) Representative Western blot and analysis of HDAC4 expression levels in hiPSCMs subjected to different experimental treatments. All quantifications are derived from n = 5 independent assays/group, PCR experiments were performed with two replicates each. All quantitative data are presented as mean ± SEM. ***$p < 0.001$ determined by one-way ANOVA followed by post hoc tests with Bonferroni correction. Abbreviations have been previously described.

3.- Data analysis obtained from the STRING database (http://string-db.org/), allowed us to determine that YY1 interacts with HDAC4 in the murine heart with a score of 0.93.

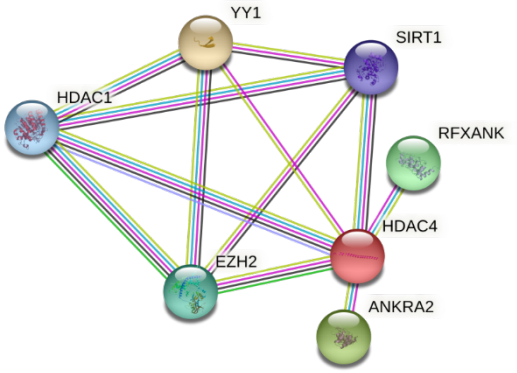

Figure S3.

YY1 interacts with HDAC4 in murine hearts.

4.-

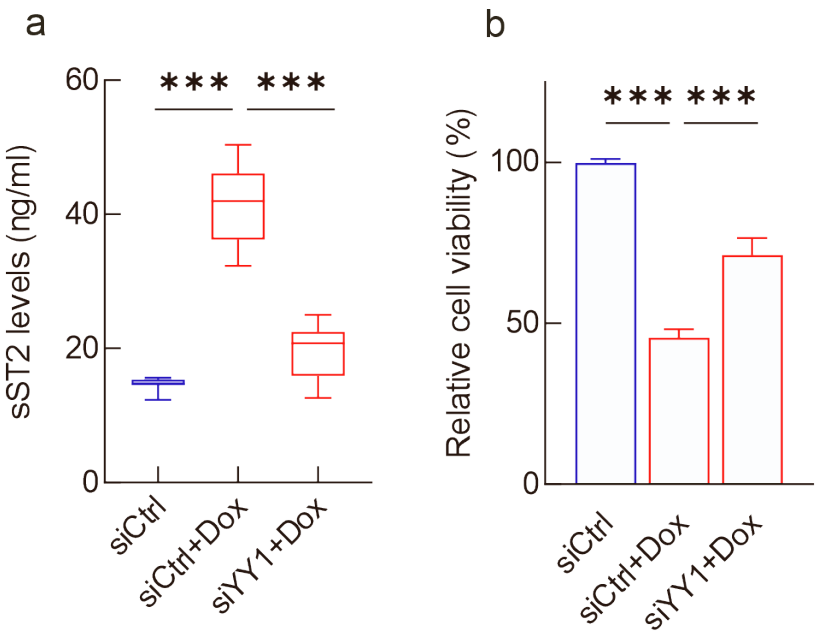

Figure S4.

Silencing of YY1 prevents Dox from affecting sST2 protein levels which leads to improved cell viability. (a) Measurement of sST2 levels in supernatants obtained from hiPSCMs exposed to 5 μM Dox for 15 h under different experimental conditions. (b) Cellular viability of hiPSCMs exposed to 5 μM Dox for 15 h under different experimental conditions. All quantifications are derived from n = 5 independent assays/group. All quantitative data are presented as mean ± SEM. ***p < 0.001 determined by one-way ANOVA followed by post hoc tests with Bonferroni correction. Abbreviations as before.

5.-

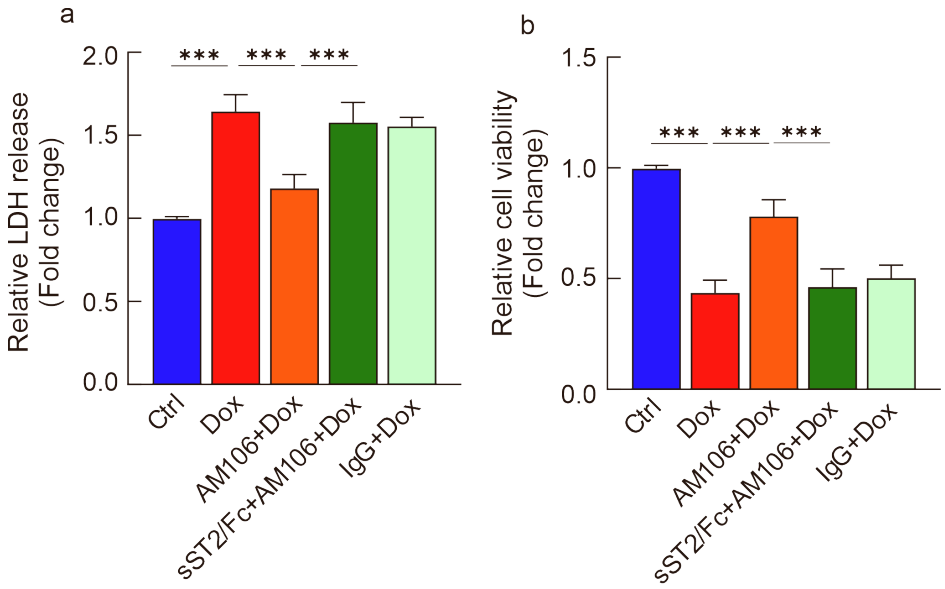

Figure S5.

The addition of sST2 blocks the preventive effect of AM106 in hiPSCMs treated with 5 μM Dox for 15 h. (a) LDH levels measured in supernatants obtained from hiPSCMs exposed to different experimental treatments. (b) Cellular viability of hiPSCMs exposed to different experimental treatments. All quantifications are derived from n = 5 independent assays/group. All quantitative data are presented as mean ± SEM. ***p < 0.001 determined by one-way ANOVA followed by post hoc tests with Bonferroni correction. Abbreviations: LDH: lactate dehydrogenase; sST2/Fc: soluble ST2 isoform Fc fusion protein. Others abbreviations as before.

6.- Animals that received *AM106* treatment showed an improved ejection fraction, compared to control animals that were treated with AC, suggesting prevention from Dox-induced cardiotoxicity based on muscle mass increase (panel a). Indeed, left ventricular (LV) mass was significantly decreased with Dox, but this was partially prevented in the AM106b group (panel b). Similarly, LV volume was significantly increased with Dox, while mice with *AM106* treatment were protected from Dox-induced cardiotoxicity (panel c). The wall thickness of the myocardium, another parameter for atrophy, was significantly decreased with Dox (panel d), whereas *AM106* treatment moderately increased muscle thickness (panels d and e). Interestingly, mice exposed to *PR55α protector* showed similar results to those mice treated with *AM106*, even in the presence of Dox.

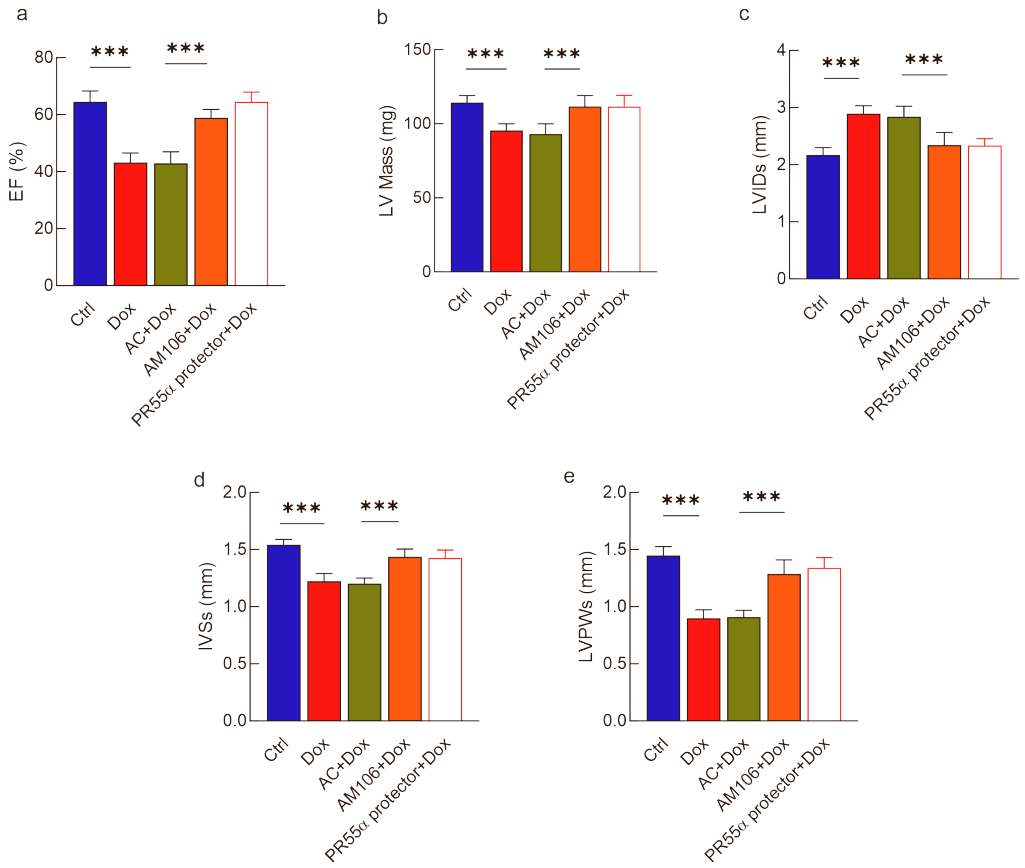

Figure S6.

AM106 treatment prevents cardiac dysfunction in mice treated with Dox. Echocardiographic analyses of control hearts (n = 10), hearts with Dox (n = 10), *AC*-hearts exposed to Dox (n=10), *AM106* hearts exposed to Dox (n = 10), and *PR55α protector* hearts exposed to Dox (n=10) showing ejection fraction (a), left ventricular mass (b), left ventricular internal diameter systole (c), interventricular septum systole (d), and left ventricular posterior wall thickness systole (e). All quantifications were derived from n = 10 mice/group, and PCR experiments were performed with two replicates each. All quantitative data are presented as mean ± SEM. ***$p < 0.001$ determined by one-way ANOVA followed by post hoc tests with Bonferroni correction. The echocardiographic procedure was performed by a blinded trained investigator, following the protocol of the Echocardiography Committee of the Specialty of Cardiology of the American College of Veterinary Internal Medicine and the American Society of Echocardiography recommendations[1,2].

7.-

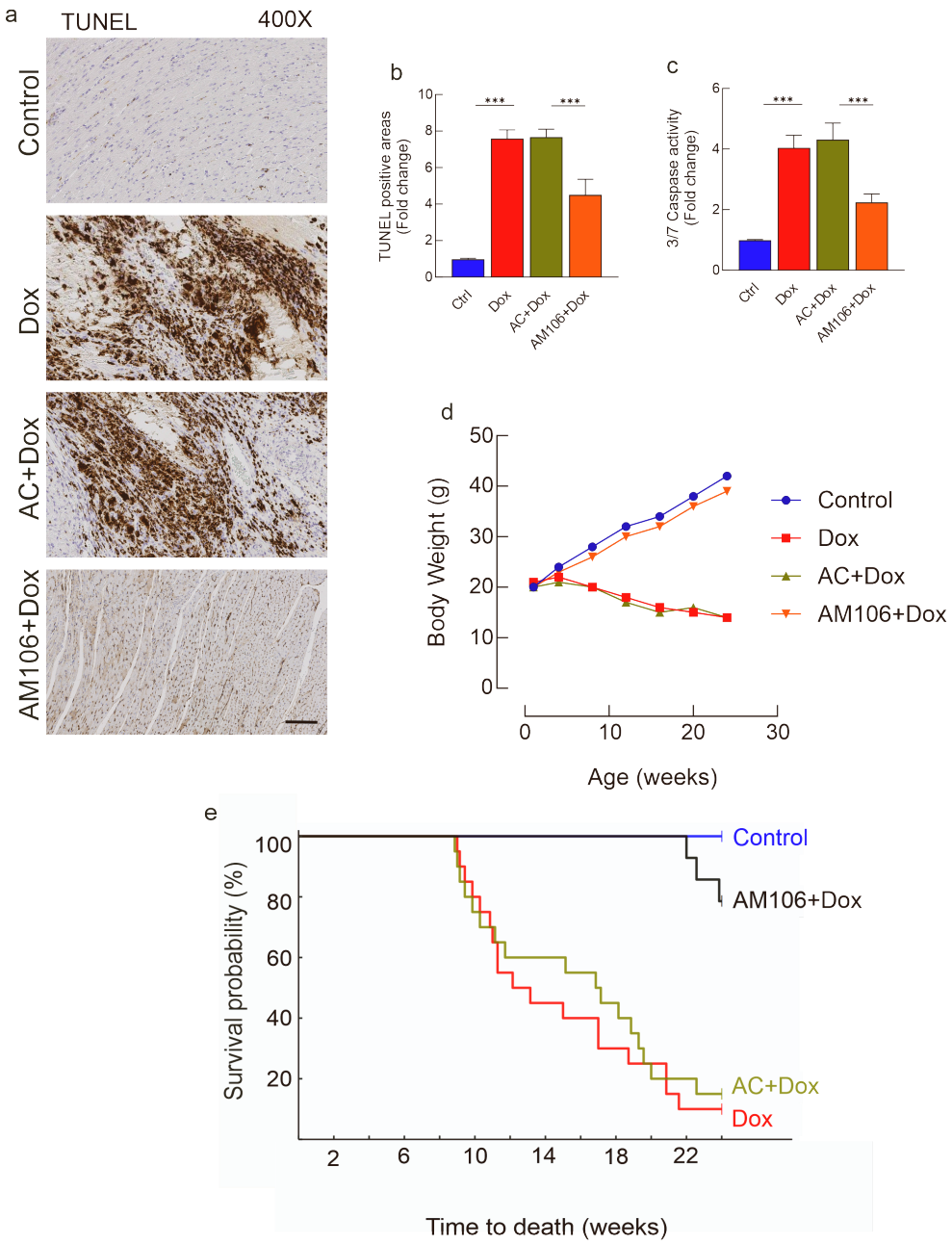

Figure S7.

AM106 treatment in LV myocardium tissue prevents apoptosis, whole-body cachexia and increased mortality associated with Dox treatment. (a-c) Representative microphotographs; scale-bar: 100 μm (a), analysis of TUNEL staining (b) and caspases 3/7 activity measurements (c) obtained from LV myocardium tissue, under different

experimental procedures. (d) Body weight kinetic from mice under different treatments. (e) Survival probability kinetic from mice under different treatments. All quantifications were derived from n = 10 mice/group. All quantitative data are presented as mean ± SEM. ***$p < 0.001$ determined by one-way ANOVA followed by post hoc tests with Bonferroni correction. Kaplan-Meier curves and pairwise comparisons between groups using a log-rank test. Abbreviations as before.

8.-

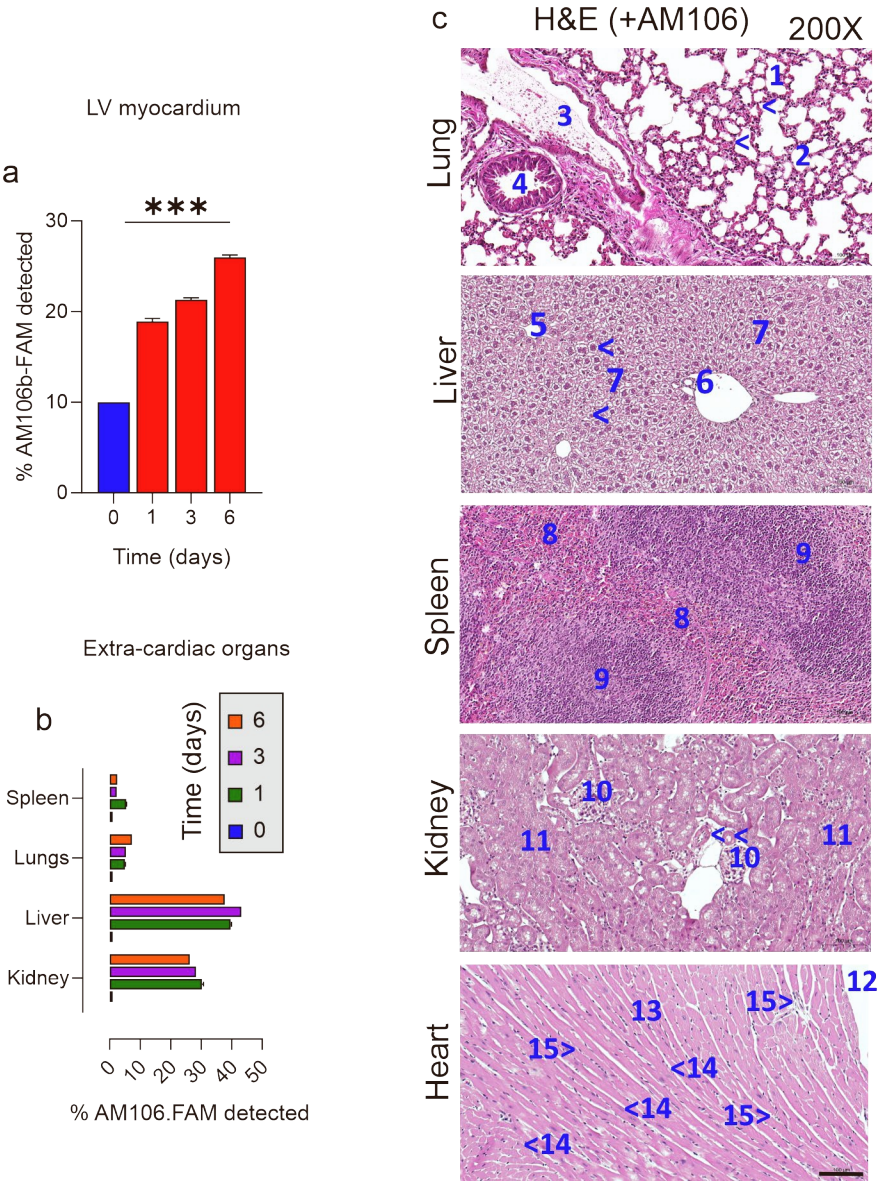

Figure S8.

AM106b biodistribution and safety. Accumulation of *AM106* in time-manner at myocardium (a) and extra-cardiac organs (b). (c) Histopathologic images at 8 weeks in mice treated with AM106b. Scale-bar: 100 µm All quantifications are derived from n = 5 mice/group. All quantitative data are presented as mean ± SEM. ***p < 0.001 determined by one-way ANOVA followed by post hoc tests with Bonferroni correction.

Specific comments for safety (Figure S8, panel c).

LUNG: the alveoli (1), airways (2) and vessels (3) showed a normal appearance, with no histopathologic alterations or cellular infiltrates. Only slight congestion (head arrows) could be identified within alveolar walls.

LIVER: The histopathologic examination of the liver revealed no significant alterations. Centrilobular vein (5), portal tracts (6), sinusoids (head arrows) and hepatocytes (7) showed a normal appearance.

SPLEEN: Examination of the spleen revealed no histopathologic alterations. The red pulp (8) and lymphoid follicles of the White pulp (9) showed a normal structure.

KIDNEY: Regarding the kidney and similarly to the other organs, no histopathologic features were observed. Thus, medullar glomeruli (10), renal tubules (11) and vessels (head arrows) showed normal appearance, with no significant alterations or cellular infiltrates. Hematoxylin and eosin stain.

HEART: Micrograph obtained from the left ventricle. Visual analysis of heart samples showed no histopathologic alterations neither ventricular cavity (12) nor ventricular wall (13), in which cardiomyocytes (14) and vessels (15) showed a normal appearance with no signs of celular alterations, extracelular deposits or cellular infiltration.

9.-

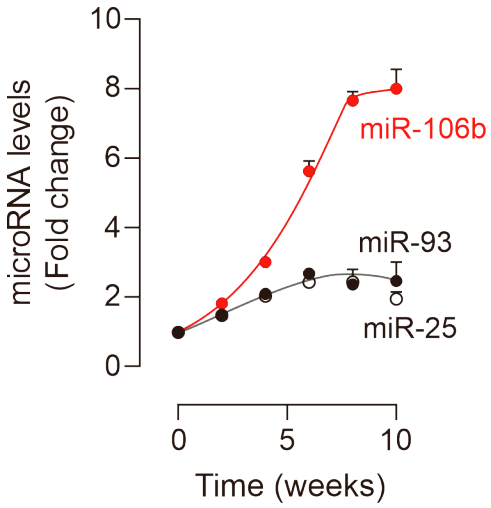

Figure S9.

Dox treatment modified the miR-106b-25 cluster levels in the LV myocardium. Levels of *miR-106b*, *miR-93*, and *miR-25* (normalized to U6) in LV myocardium from mice treated with Dox up to 10 weeks. All quantifications were derived from n = 5 mice/group, and PCR experiments were performed with two replicates each. Quantitative data are presented as mean ± SEM. ***p < 0.001 determined by one-way ANOVA followed by post hoc tests with Bonferroni correction. Others abbreviations as before.

10.-

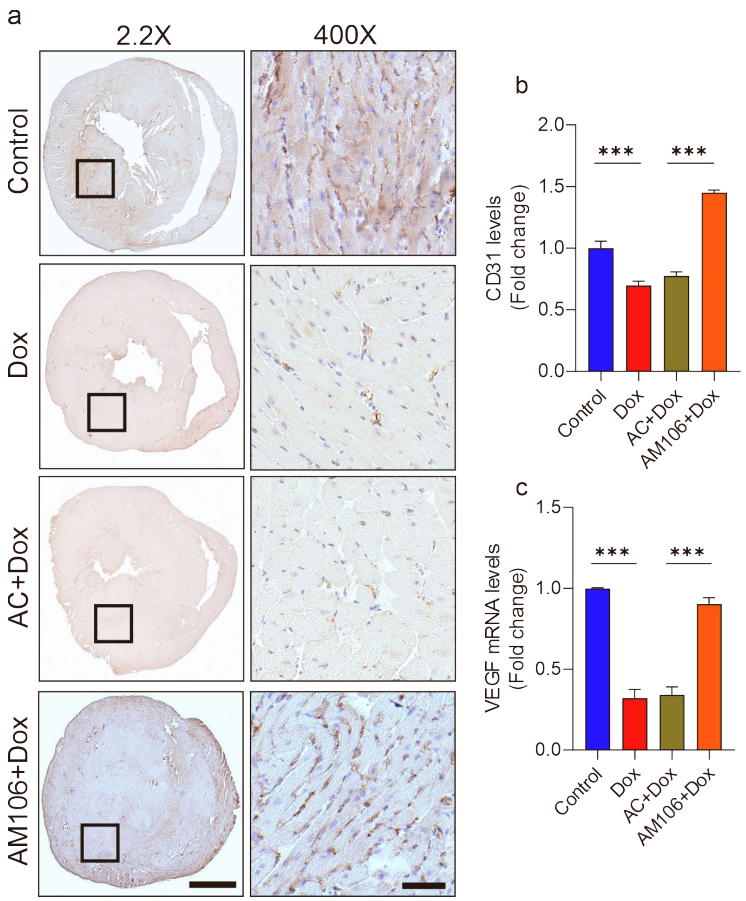

Figure S10.

AM106 treatment increases angiogenesis in LV myocardium tissue. (a) CD31-positive immunolabelling obtained from LV myocardium tissue: left column, representative images of heart sections [scale bar: 1000 μm]; right columns, representative micrographs obtained from selected square [scale bar: 50 μm]. (b) Analysis of CD31 staining in selected sections. (c) Quantitative reverse transcription polymerase chain reaction analysis of *VEGF* (normalized to GAPDH) in LV myocardium. All quantifications were derived from n = 5 mice/group, and PCR experiments were performed with two replicates each. Quantitative data are presented as mean ± SEM. ***p < 0.001 determined by one-way ANOVA followed by post hoc tests with Bonferroni correction. Abbreviations: CD31: cluster of differentiation 31; VEGF: Vascular endothelial growth factor. Other abbreviations as before.

11.-

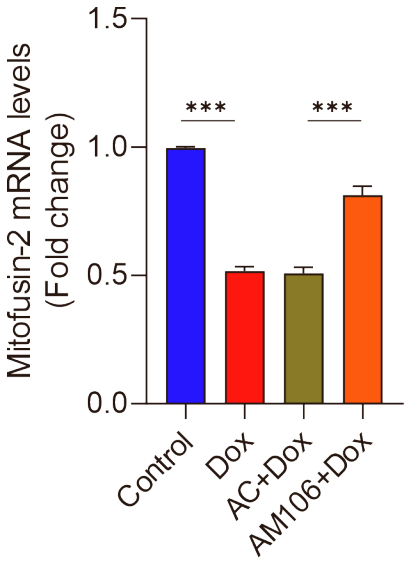

Figure S11. *AM-106 treatment prevents against Dox-induced MFN2 down-regulation in the myocardium.* Quantification of mitofusin-2 mRNA levels by RT-qPCR (normalized to GAPDH) in LV myocardium from mice treated with Dox under the experimental conditions which were detailed in the main manuscript (figure 5a). All quantifications were derived from n = 7 mice/group, and PCR experiments were performed with two replicates each. All quantitative data are presented as mean ± SEM. ***p < 0.001 determined by one-way ANOVA followed by post hoc tests with Bonferroni correction.

12.-

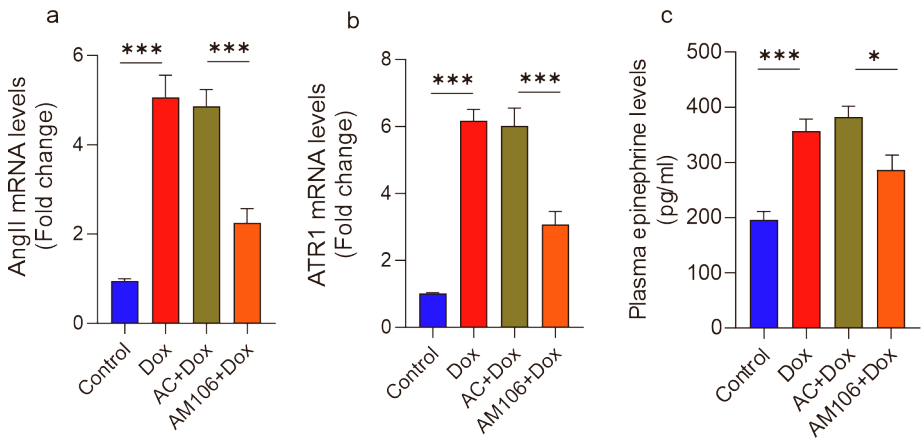

Figure S12. *Effect of AM106b treatment on AngII, AT1R and epinephrine levels in LV myocardium from mice.* Quantitative reverse transcription polymerase chain reaction analysis of *AngII* (a), *AT1R* (b) mRNA levels (normalized to GAPDH) in LV myocardium. (c) Serum epinephrine levels. All quantifications were derived from n = 5 mice/group, and PCR experiments were performed with two replicates each. Quantitative data are presented as mean ± SEM. ***p < 0.001, *p<0.05 determined by one-way ANOVA followed by post hoc tests with Bonferroni correction.

13.-

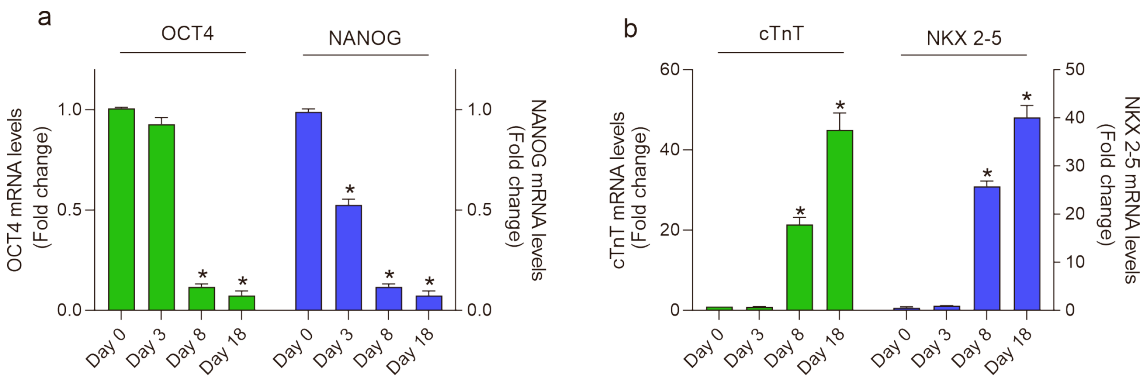

Figure S13.

Relative gene expression of pluripotency (a) and cardiac-specific markers (b) in hiPSCMs. The mean Ct values of triplicate measurements were normalized against the values for *GAPDH* for the same sample. Following normalization, the means of three independent assays were plotted, and the data represented are the mean ± SEM. * $p<0.001$ with respect to day 0. determined by one-way ANOVA followed by post hoc tests with Bonferroni correction.

14.-

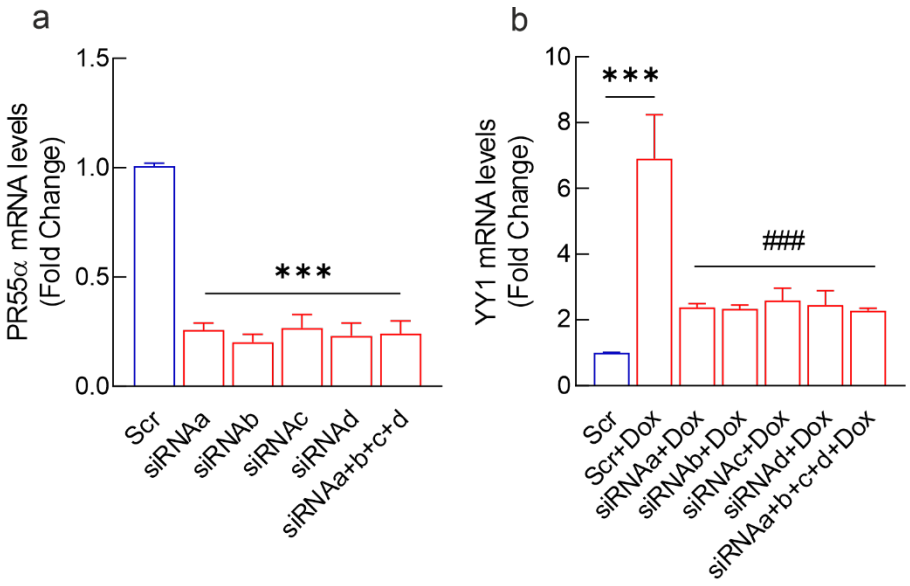

Figure S14.

SiYY1 and siPR55α transfection efficiency. HiPSCMs were preincubated with scramble siRNA (scr), with a combination of four siRNAs to *PR55α* (*siRNA PR55a*_a+b+c+d), *YY1* (*siRNA YY1*_a+b+c+d), or single siRNAs. The mRNA expression of *PR55α* (a) and *YY1* (b) was analyzed by quantitative RT-PCR (normalized to GAPDH). All quantifications are derived from n = 5 independent assays/group. All quantitative data are presented as mean ± SEM. ***p<0.001 vs control-Scr or ### p<0.001 vs Scr+Dox determined by one-way ANOVA followed by post hoc tests with Bonferroni correction. Abbreviations: Src: Scramble.

References

1. Smith, P.K., Krohn, R.I., Hermanson, G.T., Mallia, A.K., Gartner, F.H., Provenzano, M.D., Fujimoto, E.K., Goeke, N.M., Olson, B.J., and Klenk, D.C. (1985). Measurement of protein using bicinchoninic acid. Anal. Biochem. *150*, 76–85.
2. Asensio-Lopez, M.C., Lax, A., Fernandez del Palacio, M.J., Sassi, Y., Hajjar, R.J., Januzzi, J.L., Bayes-Genis, A., and Pascual-Figal, D.A. (2019). Yin-Yang 1 transcription factor modulates ST2 expression during adverse cardiac remodeling post-myocardial infarction. J. Mol. Cell. Cardiol. *130*, 216–233.
3. Asensio-Lopez, M.C., Sassi, Y., Soler, F., Fernandez del Palacio, M.J., Pascual-Figal, D., and Lax, A. (2021). The miRNA199a/SIRT1/P300/Yy1/sST2 signaling axis regulates adverse cardiac remodeling following MI. Sci. Rep. *11*.
4. Semete, B., Booysen, L., Lemmer, Y., Kalombo, L., Katata, L., Verschoor, J., and Swai, H.S. (2010). In vivo evaluation of the biodistribution and safety of PLGA nanoparticles as drug delivery systems. Nanomedicine Nanotechnology, Biol. Med. *6*, 662–671.